Serum starvation-induces down-regulation of Bcl-2/Bax confers apoptosis in tongue coating-related cells *in vitro*

YANHUA HUANG[1*], ZIYI FU[1*], WEI DONG[2], ZHENMING ZHANG[2], JINQUAN MU[3] and JUNFENG ZHANG[2]

[1]Department of Stomatology, Nanjing Maternity and Child Health Medical Institute,
Obstetrics and Gynecology Hospital Affiliated to Nanjing Medical University, Nanjing, Jiangsu 210029;
[2]Department of Pathogen and Immunology, Discipline of Chinese and Western Integrative Medicine,
College of Basic Medicine, Nanjing University of Chinese Medicine, Nanjing, Jiangsu 210023;
[3]Department of Stomatology, Ningbo Dental Hospital, Ningbo, Zhejiang 315100, P.R. China

Abstract. Tongue squamous epithelial cells are the main component of tongue coating, with proliferation, differentiation and apoptosis being the root cause of the formation and maintenance of tongue coating. The present study aimed to explore the molecular mechanism by which serum influences tongue coating, to enable a better understanding for future investigations. Tongue carcinoma squamous cells were exposed to serum-starvation *in vitro*. Cellular proliferation and apoptosis were observed by using 3-[4,5-dimethyl-2-thiazolyl]-2,5-diphenyl-2-H-tetrazolium bromide (MTT) assay, flow cytometry, Hoechst staining, scanning electron microscope (SEM), transmission electron microscope (TEM), and by measuring the expression ratio of B-cell lymphoma 2 apoptosis regulator (Bcl-2)/Bcl-2 associated protein X apoptosis regulator (Bax) mRNA and protein by reverse transcription-quantitative polymerase chain reaction (RT-qPCR) and western blotting, respectively. MTT assays revealed that serum-starvation results in suppression of cellular proliferation, while flow cytometry data revealed that serum-starvation induces cell cycle arrest at G1 phase and increases apoptosis. In addition, chromatin condensation and membrane blebbing were observed through Hoechst staining, TEM and SEM. The Bcl-2/Bax ratio was found to be significantly decreased in cells that had undergone serum-starvation by both RT-qPCR and western blotting analysis, further indicating that serum-starvation induces apoptosis. Therefore, tongue carcinoma squamous cells in a serum-free medium can simulate apoptosis related to the formation of tongue coating, which may offer guidance for future investigations about other factors.

Introduction

Tongue analysis, one of the essential methods of traditional Chinese medicine diagnosis, helps understand pathological changes of internal organs and meridians (1). Tongue coating is the main content used for tongue analysis, and serves a role in reflecting the occurrence, development and prognosis of the disease (2). Tongue coating is a visible layer adherent to the tongue dorsum, mainly comprised of desquamated epithelial cells and four different types of papillae (3).

These features have been examined via electron microscopy studies, with the formation of the tongue coating found to be dependent on the physiological state of filiform papillae (4). For example, the filiform papillae within the cuticle of a thick coating are prominent and dense, while the cuticle of a thin coating is obviously atrophied (5). The epidermis of the tongue dorsum contains a highly specialized epithelium consisting of several stratified cell layers called squamous epithelium, with these epithelial cells continuously renewed by the mitotic activity of stem cells within the basal layer (6). Thus, the area and thickness of the tongue coating are closely associated with the proliferation, differentiation, migration and apoptosis of squamous epithelial cells.

Furthermore, some studies have shown that saliva coexists with tongue squamous epithelial cells and can affect the formation of tongue coating (7). Additionally, proteomic based research revealed that blood and saliva composition could also affect the coating (8). Another study found that levels of serum trace elements, including zinc, copper and iron, are altered in a pathological tongue coating relative to a normal control (9). In conclusion, there is a strong relationship between changes of tongue coating and serum.

Apoptosis is a controlled cell-independent death process that is regulated by protein activity and gene expression in

Correspondence to: Dr Junfeng Zhang, Department of Pathogen and Immunology, Discipline of Chinese and Western Integrative Medicine, College of Basic Medicine, Nanjing University of Chinese Medicine, 138 Xianlin Road, Nanjing, Jiangsu 210023, P.R. China
E-mail: zhangjunfeng0818@126.com

Dr Jinquan Mu, Department of Stomatology, Ningbo Dental Hospital, 1821 Ningchuan Road, Ningbo, Zhejiang 315100, P.R. China
E-mail: dentmjq@163.com

*Contributed equally

order to maintain homeostasis and adapt to environmental conditions. Unlike necrosis, apoptosis maintains a normal structure of cell organelles, cell shrinkage, chromosome condensation, DNA fragmentation, apoptosis corpuscles formation and does not cause inflammation (10). At present, gene regulation in the process of serum influencing tongue coating has not been investigated. B-cell lymphoma 2 apoptosis regulator (Bcl-2) and Bcl-2 associated protein X apoptosis regulator (Bax) are important members of the Bcl-2 gene family and are 2 of the most commonly investigated apoptosis regulators. Bcl-2 can induce cell proliferation and inhibit cell apoptosis, while Bax can accelerate apoptosis. Recent studies have shown that apoptosis hinges on the ratio of Bcl-2 and Bax in cells, with this insight providing may important clues to possible outcomes following a challenge with an apoptosis-inducing agent (11).

Thus, the present study hypothesized that serum components may be important in the formation of the tongue coating and that serum-starvation could induce epithelial cell apoptosis induced by Bcl-2/Bax in the epidermis of the tongue dorsum. To test this hypothesis and explore the molecular mechanisms of serum influencing tongue coating, an *in vitro* tongue carcinoma squamous cell culture exposed to serum-starvation was adapted to simulate apoptosis related to the formation of tongue coating. By observing the changes of cell cycle, apoptosis and Bax/Bcl-2 expression in a serum-free medium, this approach enabled the examination of the mechanisms pertaining to the formation of tongue coating and may aid in a further understanding for future investigations.

Materials and methods

Cell culture. A tongue squamous cell carcinoma cell line, Tca8113 (Ninth People's Hospital of Shanghai, Shanghai, China), was maintained in RPMI-1640 medium (Gibco; Thermo Fisher Scientific, Inc., Waltham, MA, USA) supplemented with 10% heat-inactivated fetal bovine serum (FBS; Hyclone; GE Healthcare Life Sciences, Logan, UT, USA), 100 mg/ml streptomycin and 100 U/ml penicillin (Invitrogen; Thermo Fisher Scientific, Inc., Waltham, MA, USA) in a humidified atmosphere with 5% CO_2 at 37˚C.

MTT assay. Cell viability was evaluated using a 3-(4,5-dimethylthiazol-2-yl)-2,5-diphenyltetrazolium (MTT) assay as previously described (12). Briefly, $1x10^4$ cells/well were seeded in 96-well plates and cultured for 18~24 h to reach 90% confluency. Following attachment, cells were washed twice with PBS, then serum-free medium added. Both serum deprived and control (10% serum) cells were harvested at 0, 12, 24, 36, 48 and 72 h. At each time point, the cell culture supernatants were discarded and 20 μl MTT solution was added to each well (0.5 mg/ml; Sigma Aldrich; Merck KGaA, Darmstadt, Germany), then the cells were cultured for a further 4 h. The supernatants were then removed and 200 μl DMSO was added to each well, with slight agitation for 15 min. The absorbance at a wavelength of 490 nm was then detected using a PowerWave 340 Microplate Reader (Bio-Tek Instruments, Inc., Winooski, VT, USA), with 4 replicates used for each well and a mean value calculated.

Flow cytometry analysis. Cells were seeded at $1x10^4$ cells/well in a 24-well plate and cultured for 18-24 h to reach 90% confluency. Following attachment, cells were washed two times with PBS and serum starvation was evoked. At 0, 12, 24, 36, 48 and 72 h, adherent cells were trypsinized and collected together with the medium containing non-adherent cells. Apoptosis was evaluated using an Annexin V-fluorescein isothiocyanate (FITC)/propidium iodine (PI) double staining apoptosis detection kit (MBL International Co., Woburn, MA, USA) according to the manufacturer's protocol, in conjunction with FACS Accuri C6 flow cytometer (BD Biosciences, Franklin Lakes, NJ, USA) and analyzed by using FlowJo 7.6.1 software (TreeStar, San Carlos, CA, USA). Cell-cycle analysis was also evaluated using a cell-cycle analysis kit (BD Cycletest Plus DNA kit; BD Biosciences) as described previously (13).

Hoechst staining. To assess the effects of serum-starvation on nuclear material, cells were stained with Hoechst 33342. Cells were seeded at a density of $5x10^4$ cells/well in a 24-well plate for 24 h with 6 replicates/sample. Cells were then washed 3 times with PBS and fixed with 10% paraformaldehyde for 5 min. Cells were washed with PBS before adding Hoechst working solution (10 mg/ml; Molecular Probes; Thermo Fisher Scientific, Inc.), followed by a 15 min incubation at 37˚C. Images were captured with an Olympus IXSI inverted microscope using 350 nm excitation and 450 nm emission filters. A total of 3 images per treatment replicate were captured at x10 and x20 magnifications.

Reverse transcription-quantitative polymerase chain reaction (RT-qPCR). RT-qPCR was employed to detect the mRNA expression levels of Bcl-2, Bax and the housekeeping gene glyceraldehyde-3-phosphate dehydrogenase (GAPDH). Following serum starvation, total RNA was extracted using TRIzol reagent (Invitrogen; Thermo Fisher Scientific, Inc.), according to the manufacturer's protocols. Purified total RNA (1 μg) was then reverse transcribed using a First Strand cDNA Synthesis Kit (Takara Bio, Inc., Otsu, Japan). RT-qPCR was performed with the following primers: Bax, forward 5'-GGC CCACCAGCTCTGAGCAGA-3' and reverse 5'-GCCACG TGGGCGGTCCCAAAGT-3'; Bcl-2, forward 5'-GTGGAG GAGCTCTTCAGGGA-3' and reverse 5'-AGGCACCCAGGG TGAGCAA-3' (14). PCR primers for the internal control gene GAPDH forward: 5'-GGAGAAACCTGCCAAGTATG-3' and reverse: 5'-TTACTCCTTGGAGGCCATGTAG-3' (15). Reactions were conducted in 96-well plates with a final volume of 20 μl including 10 μl SYBR Green PCR Master Mix (Invitrogen, Carlsbad, CA, USA), plus 1 μl each primer (2 μM), 1 μl template DNA, and 7 μl ddH$_2$O. Thermal cycling and fluorescence detection were conducted on ABI ViiA7 (Applied Biosystems, Thermo Fisher Scientific, Inc., Waltham, MA, USA). The reaction mixtures were cycled 35 times at 94˚C for 30 sec, 60˚C for 30 sec and 72˚C for 30 sec. Each reaction was run in triplicate. The levels of Bcl-2 and Bax gene expression were normalized to GAPDH levels using the method of $2^{-\Delta\Delta Cq}$ (16,17). PCR products were assessed by electrophoresis, with no primer-dimers observed for either the target genes or GAPDH, and the product specificities were also confirmed by melting curve analysis.

Western blotting. Bax and Bcl-2 protein expression levels were examined by western blot analysis. Proteins within the cell lysates were separated by gel electrophoresis, with protein transferred to a nitrocellulose membrane and immunoblotting performed as previously described (18). Cells were cultured for 18-24 h to reach 90% confluency. Radioimmunoprecipitation Assay lysis buffer (Qiagen, Inc., Valencia, CA, USA) was added to each cell and vortexed for 15 min at a temperature of 4°C, then centrifuged at 12,000 x g for 10 min at a temperature of 4°C. Supernatant was transferred to a new tube and determined quantitatively by Bicinchoninic acid Protein Assay kit. Protein lysates were boiled in SDS-sample buffer for 5 min, equally loaded (20 μg/lane) onto an 8% SDS-PAGE and transferred to a polyvinylidene fluoride membrane (Bio-Rad Laboratories, Inc., Hercules, CA, USA). Membranes were then blocked for 2 h in 5% milk-Tris-Buffered Saline Tween-20 (TBST) at room temperature, then incubated with either monoclonal anti-Bax (1:750; cat. no. 5023) or anti-Bcl-2 (1:750; cat. no. 4223,) or monoclonal anti-GAPDH antibodies (1:2,000; cat. no. 5174; all Cell Signaling Technology, Inc., Danvers, MA, USA). Membranes were then washed four times in TBST and incubated with appropriate horseradish peroxidase-conjugated secondary antibodies (1:1,000; cat. no. 7074; Cell Signaling Technology, Inc.). Blots were visualized by enhanced chemiluminescence (Thermo Fisher Scientific, Inc.) and analyzed using a scanning densitometer with molecular analysis software (BioSens Gel Imaging System 750, Shanghai Bio-Tech Co., Ltd., Shanghai, China).

Scanning electron microscopy (SEM). Tca8113 cells were subjected to scanning electron microscopy as previously described (19). Briefly, Tca8113 cells were exposed to serum starvation for 0, 12, 24, 36, 48 and 72 h, then fixed for scanning electron microscopy by immersion in 2.5% glutaraldehyde-PBS (pH 7.4) at room temperature for 1 h. Following fixation, samples were washed 3 times with PBS for 1 h and dehydrated in a graded series of ethanol (50, 70 and 80% at 20 min per change; 90, 96 and 100% at 15 min per change; and 100% for three changes at 4°C). Samples were then dried and imaged using a Model S-3000N scanning electron microscope (Hitachi, Ltd., Tokyo, Japan).

Transmission electron microscopy (TEM). Tca8113 cells were exposed to serum starvation for 0, 12, 24, 36, 48 and 72 h, then fixed for TEM. Samples were fixed overnight at 4°C in 0.1 M PBS buffer containing 2.5% glutaraldehyde (v/v) and post-fixed in 1% OsO_4 in the same buffer for 2 h at 4°C. The samples were then dehydrated through a graded ethanol series [30, 50, 70, 90, and 100% (v/v in ddH_2O) for 15 min at each concentration], followed by a graded ethanol:acetone series (3:1, 1:1, 1:3, and 0:1 for 15 min at each concentration) at 4°C and embedded in araldite resin. Sections (60-80 nm), which were obtained with an ultramicrotome, were stained in 3% acetic acid uranium-citric acid and viewed using an H-7650 transmission electron microscope (Hitachi, Ltd., Tokyo, Japan) (20).

Statistical analysis. All data were statistically analyzed using the SPSS 16.0 software package (SPSS Inc., Chicago, IL, USA), with results expressed as the mean ± standard deviation.
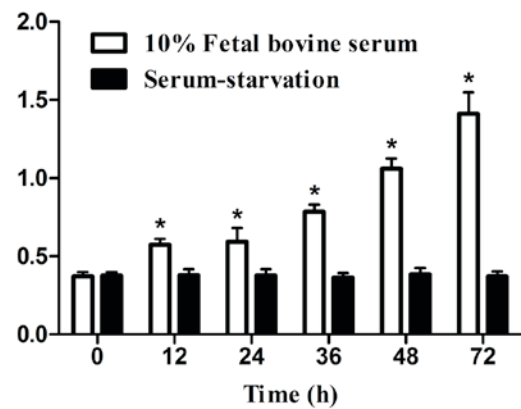

Figure 1. Suppressive effect of serum-starvation on cell proliferation, assessed by MTT assay. Data are presented as the mean ± standard deviation (n=5). *P<0.05 vs. 0 h.

The means among diverse samples were compared by one-way analysis of variance and multiple comparisons among the groups were conducted using the least-significant difference (LSD) method. Dunnett's method was employed to evaluate the heterogeneity of the variance. P<0.05 was considered to indicate a statistically significant difference.

Results

Serum-starvation suppresses cellular proliferation. Growth inhibitory effects on cellular proliferation, measured by MTT assay, are shown in Fig. 1 Compared with the 0 h control, no significant differences were observed following serum-starvation for 12, 24, 36, 48 and 72 h, cell proliferation levels (P>0.05; Fig. 1). Conversely, cell proliferation significantly increased compared with the 0 h control in medium containing 10% FBS (P<0.05; Fig. 1).

Serum-starvation induces cell cycle arrest at G1 phase. A significant and time-dependent G_1 phase arrest was noted in serum-starved cells, compared with 0 h (P<0.05; Table I and Fig. 2). A peak in this effect was reached at 24 h of treatment, when the number of cells at G_1 phase had significantly increased from 32.84% (untreated control) to 66.40%.

Effect of serum-starvation on cellular apoptosis. Apoptotic cells were examined by counting the percentage of early apoptotic cells (Annexin-V$^+$/PI$^-$) and late apoptotic cells (Annexin-V$^+$/PI$^+$). Under conditions of serum-starvation, the percentages of both early and late apoptotic cells were significantly elevated in a time-dependent fashion, compared with 0 h (P<0.05; Table II and Fig. 3). However, apoptosis did not continue to increase with treatment time: Following 24 h of treatment, the percentage of late apoptotic cells (Q2) peaked at 8.97% and then declined. The early apoptosis (Q4) rates continued to rise, dipped at 36 h, before reaching an apex at 48 h and then gradually declining.

Hoechst staining. Apoptosis is one of the major pathways that leads to cell death, therefore the effects of serum-starvation on apoptosis were further examined using the Hoechst

Table I. Serum-starvation induces cell cycle arrest at G1 phase.

Cell population (%)	Time (h)					
	0	12	24	36	48	72
G0/G1	32.84	54.82[a]	66.40[a]	58.79[a]	55.49[a]	54.10[a]
G2/M	18.43	10.80	4.44	15.13	13.43	6.96
S	48.73	34.39	29.15	26.08	31.08	38.94

[a]$P<0.05$ vs. 0 h. Data are presented as the mean ± standard deviation.

staining method. Manual observation of apoptotic cells based on cytoplasmic condensation, karyopyknosis and nuclear fragmentation revealed that the percentage of apoptotic cells increased as the duration of serum starvation increased (Fig. 4A-F). Serum-starvation for 36 h resulted in karyopyknosis (Fig. 4D), and as serum-starvation time increased further, classic characteristics of apoptosis were observed, including chromatin condensation and nuclei fragmentation. However, no nucleosomes were observed.

Effect of serum-starvation on cell surface morphological characteristics and ultrastructure. SEM was then used to study the effect of serum-starvation on cell surface morphological characteristics (Fig. 5). Control cells exhibited a uniform distribution of palpate and microvilli on their surfaces (Fig. 5A and D), while after 24 h of serum-starvation, the microvilli numbers were reduced and a smoothening of the cell surface was observed (Fig. 5B and E). After 72 h of serum-starvation, the microvilli were absent and the cell membrane showed breakage (Fig. 5C and F).

To study the effects of serum-starvation on cell ultrastructures, TEM was then performed. Control cells appeared round, had abundant organelles and normal double-membraned nuclei (Fig. 6A). Following serum-starvation, the nuclear membrane was domed outward with a sharp angle, the chromatin within the nuclei was concentrated and clustered on the inner border of cells and cell blebbing became visible (Fig. 6B-F).

Effects of serum starvation on Bcl-2 and Bax expression. In order to investigate the effects of serum-starvation on cellular apoptosis, Bcl-2 and Bax mRNA and protein expression was examined. Owing to the opposite effects of Bcl-2 and Bax on apoptosis, the ratio of Bcl-2/Bax was calculated. Relative to the 0 h control group, the ratio of Bcl-2/Bax was increasingly decreased after 12, 24 and 36 h serum-starvation ($P<0.05$; Fig. 7). These results suggest that serum-deprivation induces cellular apoptosis in a time-dependent manner.

Discussion

Changes to the tongue coating may reflect the condition of vitality and pathogen status in the body. Tongue squamous epithelial cells are the main component of the tongue coating, with proliferation, differentiation and apoptosis being the root cause of the formation and maintenance of tongue coating (21).
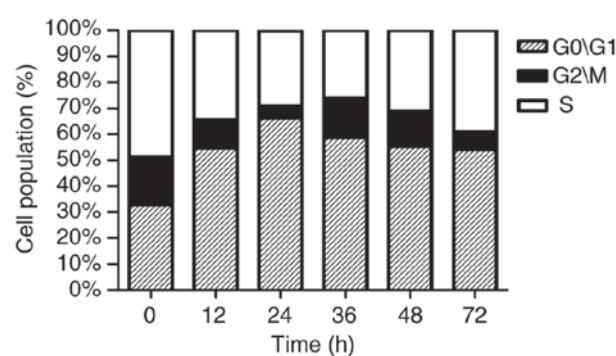

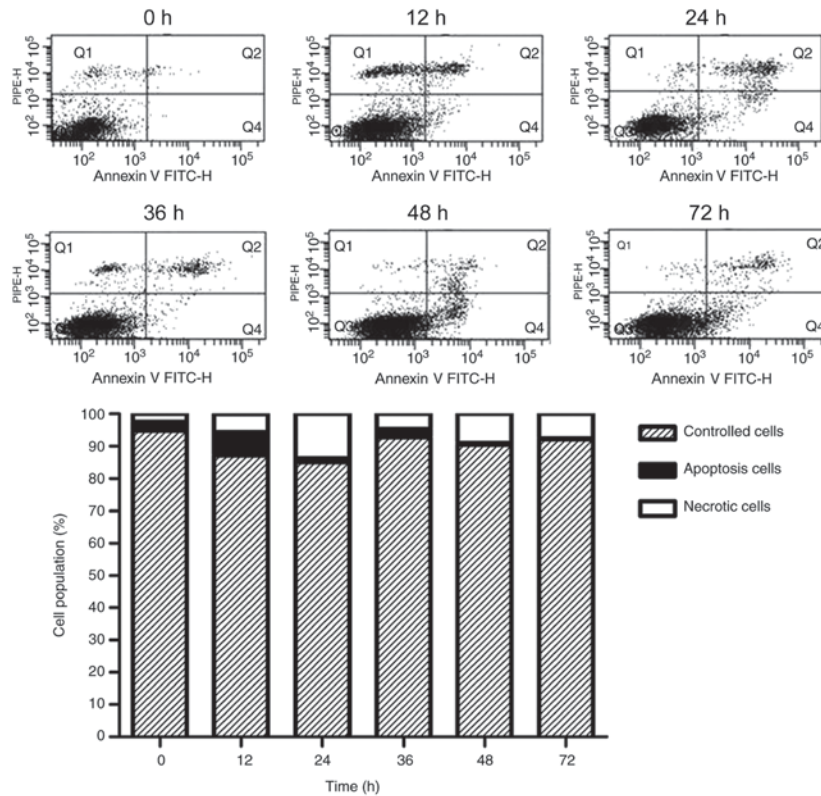Figure 2. Cell cycle analysis of cells treated with serum-starvation for 0, 12, 24, 36, 48 and 72 h. Data are presented as the mean ± standard deviation (n=5).

Therefore, examination of the mechanisms of the formation of tongue coating is meaningful at the cellular level.

However, very little research pertaining to cell function related to tongue coating formation has been examined, mainly due to: i) The oral environment being a contaminated environment, with a low cultivation success rate; ii) it is generally more difficult to obtain normal human tongue back mucosal epithelial materials because submucous tissue cannot be completely cleaned, which causes the epithelial cells to develop synchronously inside fibroblasts to different degrees (22); and iii) epithelial cells are challenging to grow in general synthetic media because they have extremely complex nutritional requirements which are not fully achievable in a uniform culturing condition (23).

Current research has found that tongue carcinoma squamous cells, which share a source in common with tongue papillary squamous epithelial cells, cultured *in vitro* can imitate the biological traits of the epithelial cell in the tongue dorsum (24). Therefore, the present study aimed to simulate tongue coating cell apoptosis by culturing tongue carcinoma squamous cells in a serum-starvation environment *in vitro*, to provide a theoretical basis for clarification of the molecular mechanisms relating to the formation of tongue coating.

There are an increasing number of reports detailing the influence of serum-starvation on cells. An increase in cell apoptosis has been observed in some cell types following serum deprivation. For example, goat skin fibroblast apoptosis was enhanced by 3- and 10-fold following 48 and 120 h serum starvation, respectively (25). In the present study, the cellular

Table II. Effect of serum-starvation on cellular apoptosis.

	Time (h)					
	0	12	24	36	48	72
Late-apoptotic cells (Q2)	0.87±0.34	4.33±1.96[a]	8.97±2.72[a]	4.67±1.45[a]	2.50±0.45[a]	2.77±0.34[a]
Early apoptotic cells (Q4)	0.23±0.09	2.63±1.25[a]	5.57±1.61[a]	1.00±0.42[a]	7.00±0.99[a]	3.90±1.27[a]

[a]$P<0.05$ vs. 0 h. Data are presented as the mean ± standard deviation.

Figure 3. Apoptosis rates of cells treated with serum-starvation for 0, 12, 24, 36, 48 and 72 h. Data are presented as the mean ± standard deviation (n=5).
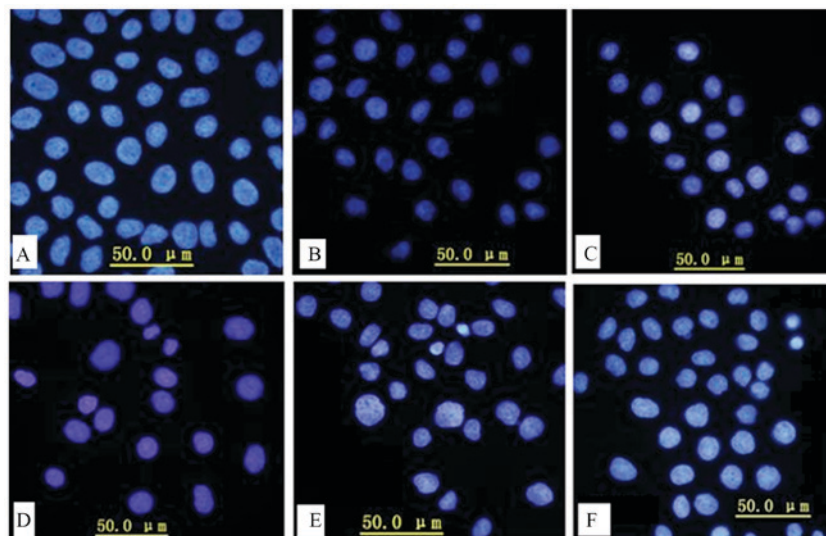

Figure 4. Hoechst staining of cells treated with serum-starvation for (A) 0, (B) 12, (C) 24, (D) 36, (E) 48 and (F) 72 h.
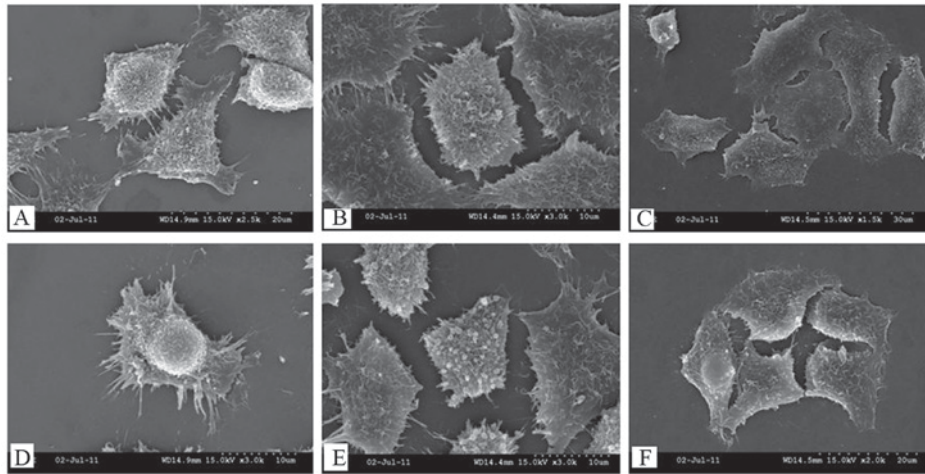
Figure 5. Surface morphological characteristics of cells following (A and D) 0, (B and E) 24 and (C and F) 72 h of serum-starvation, detected by scanning electron microscopy. (A) Synapse connections (magnification, x2500) and (D) a uniform distribution of microvilli on their surfaces (magnification, x3,000) among control cells. After 24 h of serum-starvation, (B) the microvilli numbers were reduced (magnification, x3,000) and (E) a smoothening of the cell surface was observed (magnification, x3,000). After 72 h of serum-starvation, (C) the cell membrane showed breakage (magnification, x1,500) and (F) the microvilli were absent (magnification, x2,000).
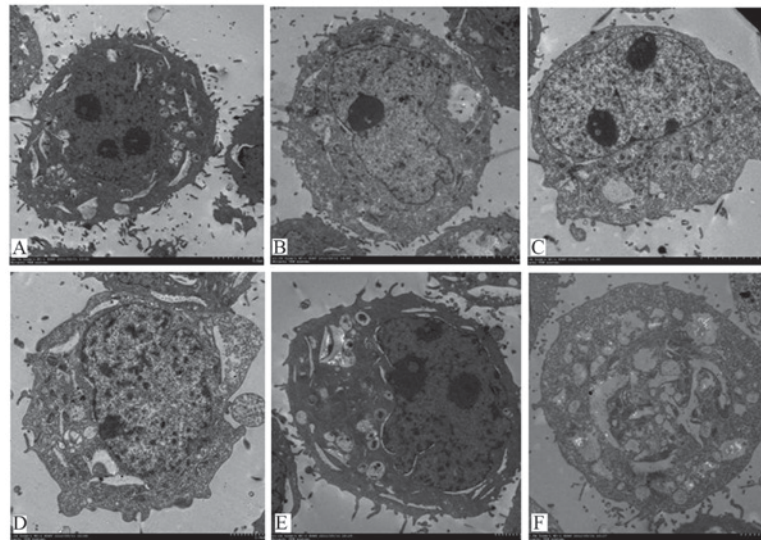

Figure 6. Ultrastructure morphological characteristics of cells following (A) 0, (B) 12, (C) 24, (D) 36, (E) 48 and (F) 72 h of serum-starvation, detected by transmission electron microscopy (magnification, x1,000).
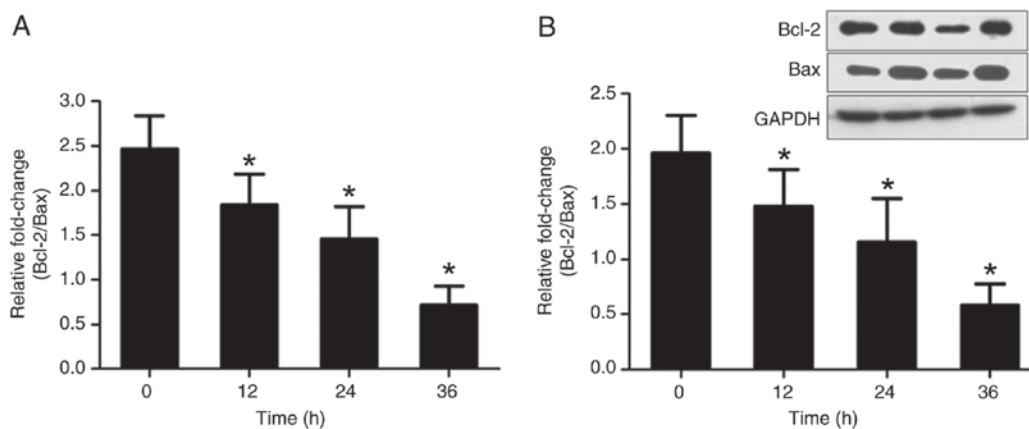

Figure 7. Bcl-2/Bax mRNA and protein expression following 0, 12, 24 and 36 h serum-starvation. (A) Bcl-2/Bax mRNA expression levels evaluated by reverse transcription-quantitative polymerase chain reaction. (B) Bcl-2/Bax protein expression evaluated by western blot assays. Data are presented as the mean ± standard deviation (n=5). *P<0.05 vs. 0 h. Bcl-2, B-cell lymphoma 2 apoptosis regulator; Bax, Bcl-2 associated protein X apoptosis regulator.

proliferative capability was estimated by the MTT method. In medium containing 10% serum, tongue carcinoma squamous cells continued to proliferate, but stopped proliferating in serum-free medium.

Based on these findings, cell cycle and apoptosis were examined by flow cytometry. As the duration of serum-starvation increased, G_0/G_1 cell cycle arrest was induced, with an apex reached at 24 h and then gradually reduced, suggesting that there could be other factors at work. Tongue squamous cancer cells showed both early and late apoptosis following serum-starvation. Early apoptotic rates increased to a peak at 24 h and then decreased, while late apoptotic rates continued to rise, but with a slight decline at 36 h, and reached an apex at 48 h, followed by a gradual decline. Examination of cells under an inverted microscope showed cellular shrinkage, rounding and a gradual loss of adherence, with the majority of cells floating after 36 h of serum-starvation. This could be due to the late apoptotic cell disruption between 24-36 h, which is consistent with the G_0 cell percentage gradually declining after 24 h, with G_0 arrest beginning to be relieved.

Morphological observations are considered the golden standard for identification of apoptotic cells, with indicators of apoptotic cells including chromatin condensation, nuclear membrane dissociation, chromatin dividing into blocks and the formation of apoptotic bodies. In the present experiments, Hoechst fluorescence microscope, TEM and SEM were applied to observe structural changes in tongue carcinoma squamous cells between experimental and control groups. These results showed that over time the percentage of apoptotic cells increased significantly, with characteristic changes noted. TEM observations demonstrated half-moon-shaped vacuoles appearing within the cells following 48 and 72 h of serum-starvation, which is due to the cells crimping when scraped with a cell knife. The results of this study concur with previous findings and visually confirmed that serum-starvation does have a role in inducing tongue squamous cancer cell apoptosis in a time-dependent manner.

In addition, the present study observed that the ratio of Bcl-2/Bax was altered in favor of apoptosis in serum-starved samples. This experimental result is consistent with the result of Papa et al (26), who observed that a down-regulation in the ratio of Bcl-2/Bax was associated with apoptosis resistance as compared to normal keratinocytes. Therefore, we speculate that the apoptosis-inducing effects might be due to a change in the mitochondrial membrane potential through the inhibition of Bcl-2 expression and/or increased expression of Bax. These results, combined with the results of MTT and flow cytometric analysis, indicate that serum-starvation could reduce the Bcl-2/Bax ratio and promote apoptosis, which is consistent with the noted inhibition of cellular proliferation.

Taken together, tongue squamous cell carcinoma cells in a serum-free medium may be used to simulate apoptosis related to the formation of tongue coating, which can offer guidance for future investigations about other factors.

Acknowledgements

References

1. Jiang B, Liang X, Chen Y, Ma T, Liu L, Li J, Jiang R, Chen T, Zhang X and Li S: Integrating next-generation sequencing and traditional tongue diagnosis to determine tongue coating microbiome. Sci Rep 2: 936, 2012.
2. Zhao Y, Gou XJ, Dai JY, Peng JH, Feng Q, Sun SJ, Cao HJ, Zheng NN, Fang JW, Jiang J, et al: Differences in metabolites of different tongue coatings in patients with chronic hepatitis B. Evid Based Complement Alternat Med 2013: 204908, 2013.
3. Singha KB, Konar S, Mondal MK and Das J: Scanning electron microscopic study of the human fungiform papillae. J Anat Soc India 59: 154-157, 2010.
4. Jackowiak H and Godynicki S: The scanning electron microscopic study of lingual papillae in the silver fox (Vulpes vulpes fulva, Desmarest, 1820). Ann Anat 186: 179-183, 2004.
5. Kawasaki K, Porntaveetus T, Oommen S, Ghafoor S, Kawasaki M, Otsuka-Tanaka Y, Blackburn J, Kessler JA, Sharpe PT and Ohazama A: Bmp signalling in filiform tongue papillae development. Arch Oral Biol 57: 805-813, 2012.
6. Da Silva AE, Rados PV, Da Silva Lauxen I, Gedoz L, Villarinho EA and Fontanella V: Nuclear changes in tongue epithelial cells following panoramic radiography. Mutat Res 632: 121-125, 2007.
7. Gonçalves AS, Arantes DA, Bernardes VF, Jaeger F, Silva JM, Silva TA, Aguiar MC and Batista AC: Immunosuppressive mediators of oral squamous cell carcinoma in tumour samples and saliva. Hum Immunol 76: 52-58, 2015.
8. Zhang A, Sun H, Wang P and Wang X: Salivary proteomics in biomedical research. Clin Chim Acta 415: 261-265, 2013.
9. Sun ZM, Zhao J, Qian P, Wang YQ, Zhang WF, Guo CR, Pang XY, Wang SC, Li FF and Li Q: Metabolic markers and microecological characteristics of tongue coating in patients with chronic gastritis. BMC Complement Altern Med 13: 227, 2013.
10. Pérez-Garijo A and Steller H: Spreading the word: Non-autonomous effects of apoptosis during development, regeneration and disease. Development 142: 3253-3262, 2015.
11. Martin LJ: Neuronal cell death in nervous system development, disease, and injury (Review). Int J Mol Med 7: 455-478, 2001.
12. Mosmann T: Rapid colorimetric assay for cellular growth and survival: Application to proliferation and cytotoxicity assays. J Immunol Methods 65: 55-63, 1983.
13. Ozeki N, Mogi M, Nakamura H and Togari A: Differential expression of the Fas-Fas ligand system on cytokine-induced apoptotic cell death in mouse osteoblastic cells. Arch Oral Biol 47: 511-517, 2002.
14. Tano T, Okamoto M, Kan S, Nakashiro K, Shimodaira S, Koido S, Homma S, Sato M, Fujita T, Kawakami Y and Hamakawa H: Prognostic impact of expression of Bcl-2 and Bax genes in circulating immune cells derived from patients with head and neck carcinoma. Neoplasia 15: 305-314, 2013.
15. Jiang W, Wang Q, Chen S, Gao S, Song L, Liu P and Huang W: Influenza A virus NS1 induces G0/G1 cell cycle arrest by inhibiting the expression and activity of RhoA protein. J Virol 87: 3039-3052, 2013.
16. Zhang W, Wang F, Xu P, Miao C, Zeng X, Cui X, Lu C, Xie H, Yin H, Chen F, et al: Perfluorooctanoic acid stimulates breast cancer cells invasion and up-regulates matrix metalloproteinase-2/-9 expression mediated by activating NF-κB. Toxicol Lett 229: 118-125, 2014.
17. Livak KJ and Schmittgen TD: Analysis of relative gene expression data using real-time quantitative PCR and the 2(-Delta Delta C(T)) method. Methods 25: 402-408, 2001.
18. Cerella C, Sobolewski C, Chateauvieux S, Henry E, Schnekenburger M, Ghelfi J, Dicato M and Diederich M: COX-2 inhibitors block chemotherapeutic agent-induced apoptosis prior to commitment in hematopoietic cancer cells. Biochem Pharmacol 82: 1277-1290, 2011.
19. Brunk UT, Dalen H, Roberg K and Hellquist HB: Photo-oxidative disruption of lysosomal membranes causes apoptosis of cultured human fibroblasts. Free Radic Biol Med 23: 616-626, 1997.
20. Zhang H, An X, Zhou Y, Zhang B, Zhang S, Li D, Chen Z, Li Y, Bai S, Lv J, et al: Effect of oxidative stress induced by Brevibacterium sp. BS01 on a HAB causing species-Alexandrium tamarense. PLoS One 8: e63018, 2013.

21. Izumi K, Nakajima T, Maeda T, Cheng J and Saku T: Adenosquamous carcinoma of the tongue: Report of a case with histochemical, immunohistochemical, and ultrastructural study and review of the literature. Oral Surg Oral Med Oral Pathol Oral Radiol Endod 85: 178-184, 1998.
22. Görögh T, Lippert BM, Gottschlich S, Folz B and Werner JA: Establishment and characterization of 2 cell lines of squamous epithelial carcinoma of the mouth floor and tongue. Laryngorhinootologie 74: 684-690, 1995.
23. Chen AK, Reuveny S and Oh SK: Application of human mesenchymal and pluripotent stem cell microcarrier cultures in cellular therapy: Achievements and future direction. Biotechnol Adv 31: 1032-1046, 2013.
24. Wilmarth PA, Riviere MA, Rustvold DL, Lauten JD, Madden TE and David LL: Two-dimensional liquid chromatography study of the human whole saliva proteome. J Proteome Res 3: 1017-1023, 2004.
25. Yu YS, Sun XS, Jiang HN, Han Y, Zhao CB and Tan JH: Studies of the cell cycle of in vitro cultured skin fibroblasts in goats: Work in progress. Theriogenology 59: 1277-1289, 2003.
26. Papa F, Scacco S, Vergari R, De Benedittis M, Petruzzi M, Lo Muzio L and Serpico R: Expression and subcellular distribution of Bcl-2 and BAX proteins in serum-starved human keratinocytes and mouth carcinoma epidermoid cultures. Life Sci 73: 2865-2872, 2003.